Mount Isa Halo Exercise

Aim of Exercise

Understand the halo of the Mount Isa Cu-Zn-Pb-Ag system

- Develop familiarity with available products/data

Document the data patterns which define:

- Scale and nature of outer halo
- Scale and nature of mid halo
- Scale and nature of inner halo
- Zoning within and between the Cu and Pb-Zn orebodies
- Potential vectoring arising from this
- Fertility vs background – ie what confirms “system” presence

Assess the scale and geometry of the halo

- Size
- Asymmetry
- Implications for exploration strategies

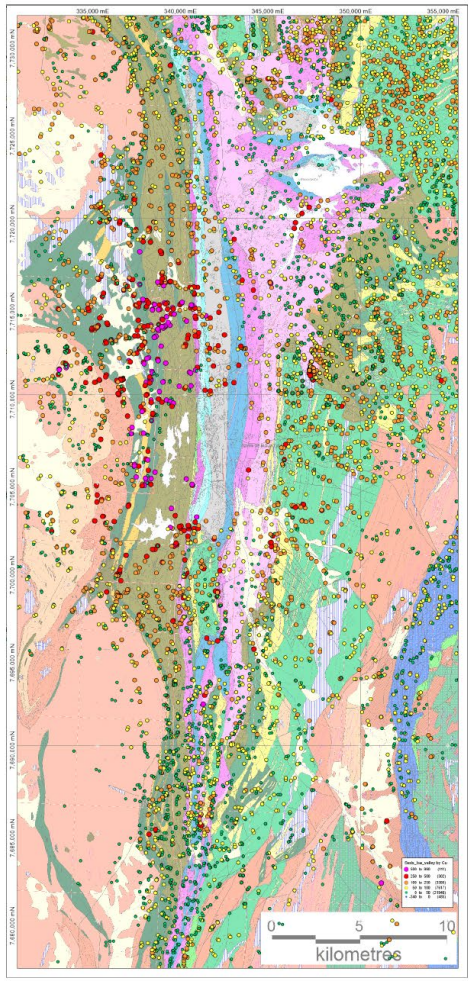

Figure 2.20. Thematic plot of stream sediment Cu values from the 2006 Mount Isa West Block Exploration Geochemistry and Drill Hole Database (QDEX 2006). Map Projection GDA94/MGA54

Figure 2.21 (facing page). Maps showing distributions of Cu, Pb and Zn in RAB and diamond drill holes (Conaghan et al. 2003). The surface projection of the Cu orebodies is also shown. Strong base metal anomalism extend more than 5km to the north of the limit of mineralisation, and copper anomalism extends south as far as the Crystallena block.

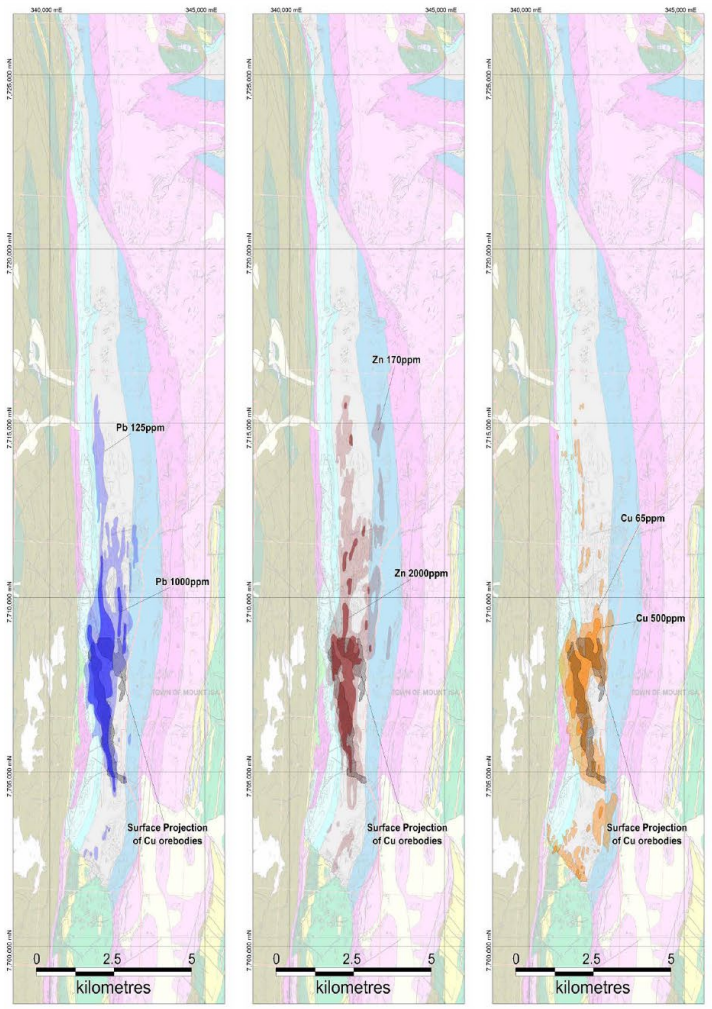

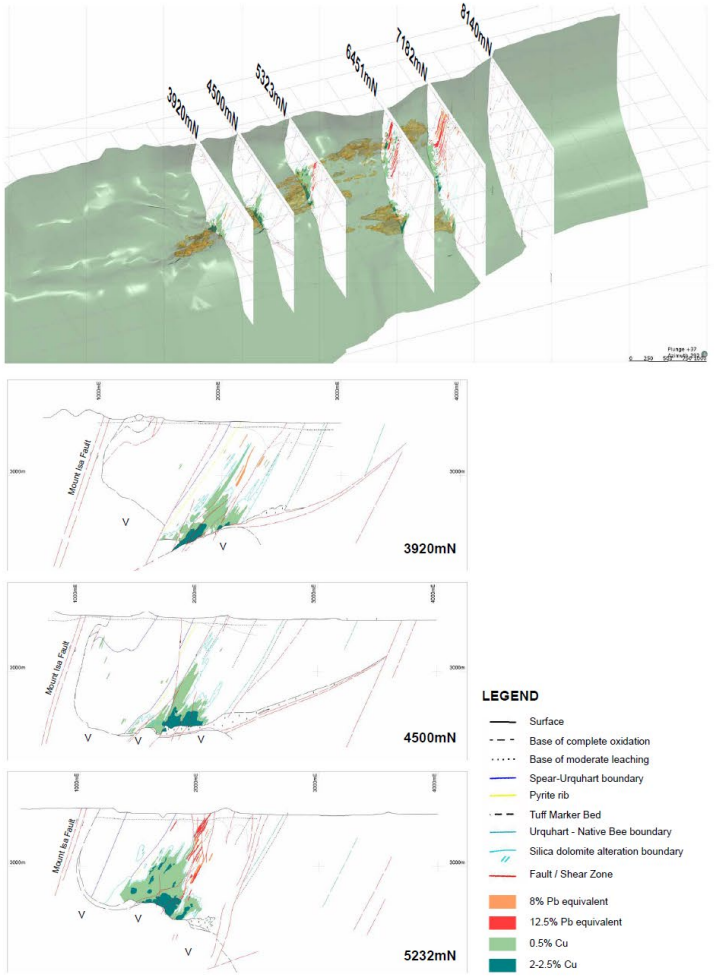

Figure 2.22. (this page and facing page). Set of sections depicting N-S variation in the geometry of Cu mineralisation, silica-dolomite alteration and lead-zinc mineralisation, and its relationship to bedding and faults. From the 1992 Mine Exploration review.

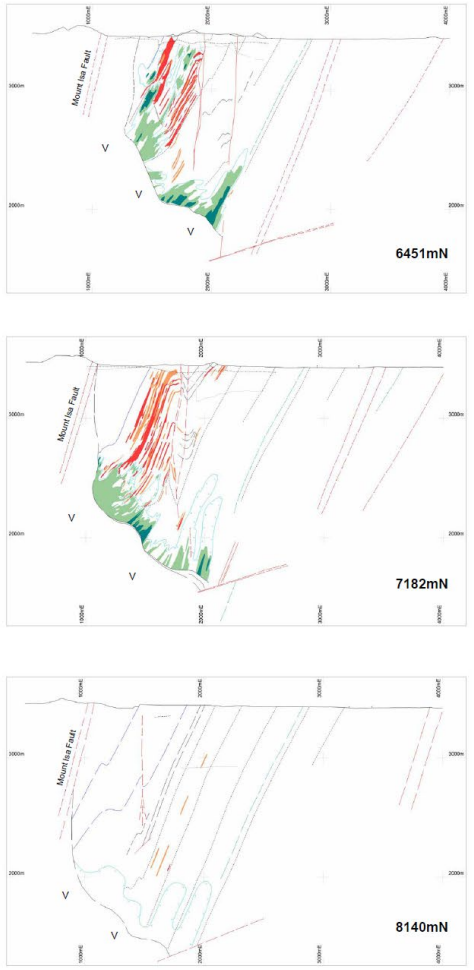

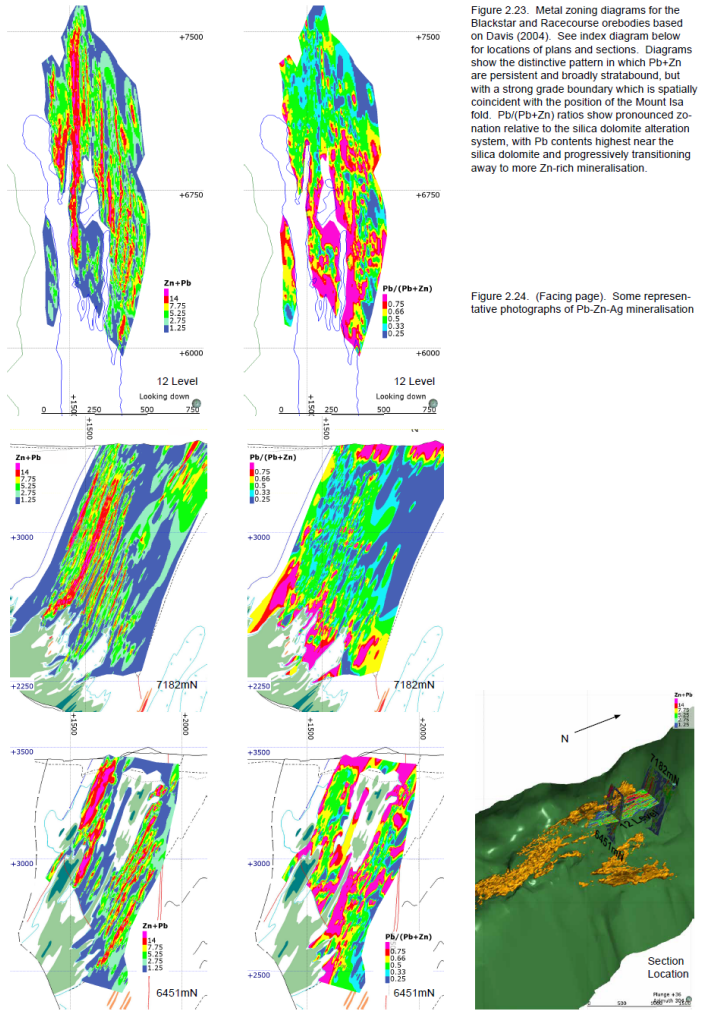

Figure 2.23. Metal zoning diagrams for the Blackstar and Racecourse orebodies based on Davis (2004). See index diagram below for locations of plans and sections. Diagrams show the distinctive pattern in which Pb+Zn are persistent and broadly stratabound, but with a strong grade boundary which is spatially coincident with the position of the Mount Isa fold. Pb/(Pb+Zn) ratios show pronounced zonation relative to the silica dolomite alteration system, with Pb contents highest near the silica dolomite and progressively transitioning away to more Zn-rich mineralisation.

Figure 2.24. (Facing page). Some representative photographs of Pb-Zn-Ag mineralisation


Alternating sphalerite-rich, pyrite-rich and shale layers. Unknown photographer.

Galena-rich mineralisation enveloping intensely folded and boudinaged shale layers. Unknown photographer.


Carbonate-veined tuff marker bed (not in place). Unknown photographer.


Small-scale disharmonic folds in Pb-Zn ore from the hinge of the Mount Isa fold. Unknown photographer.


Galena-rich mineralisation enveloping intensely folded and boudinaged shale layers. Unknown photographer.

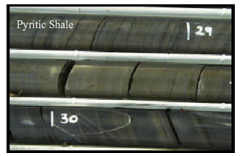

Pyritic shale. MIM AusIMM presentation.


Alternating sphalerite-rich, pyrite-rich, galena-rich and shale layers. Unknown photographer.

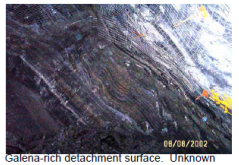
Galena-rich detachment surface. Unknown photographer.

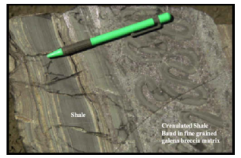
Galena-rich mineralisation enveloping intensely folded and boudinaged shale layers. MIM AusIMM presentation.

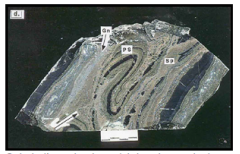
Sphalerite and galena rich bands enveloping a zone of disharmonic folding in pyritic shale. MIM AusIMM presentation

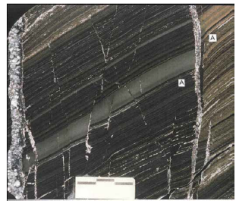
Hand specimen photograph showing a lateral transition from barren shale and siltstone to bedded sphalerite-pyrite mineralisation across a vein, strongly indicating a replacive origin for the mineralisation. Photo from Perkins (2011).


Sphalerite-rich layers occurring between folded and boudinaged pyritic shale layers, associated with coarse grained carbonate. MIM AusIMM presentation


Galena-rich mineralisation associated with weakly folded and boudinaged shale layers. Unknown photographer.

Mineralogical and chemical summary zoning from Painter (2003) PhD Thesis - Figure 2.27

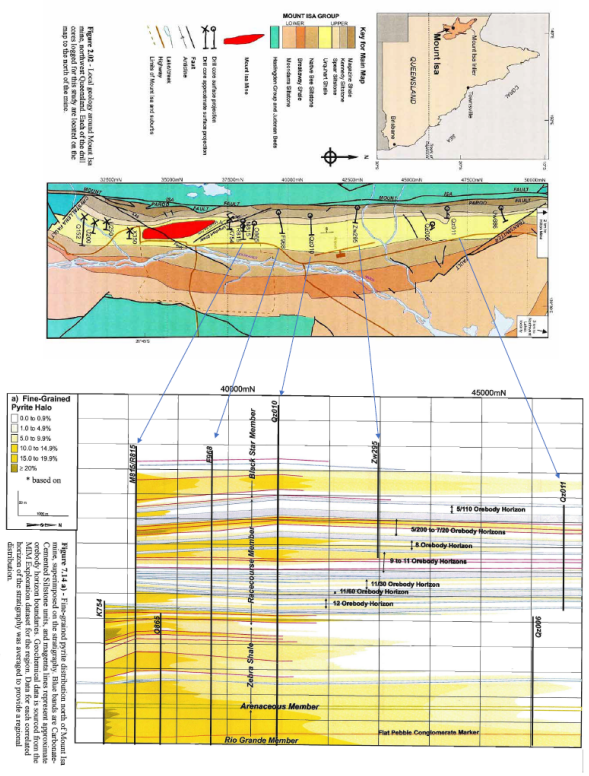

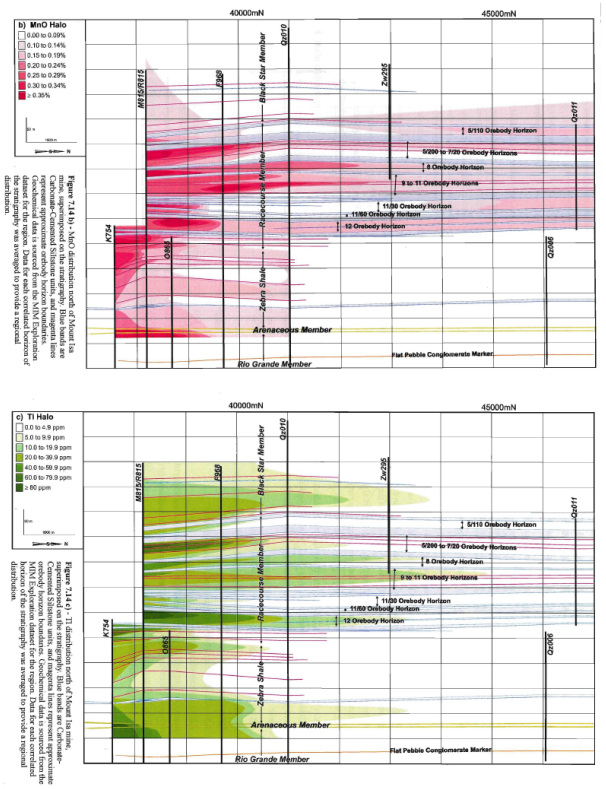

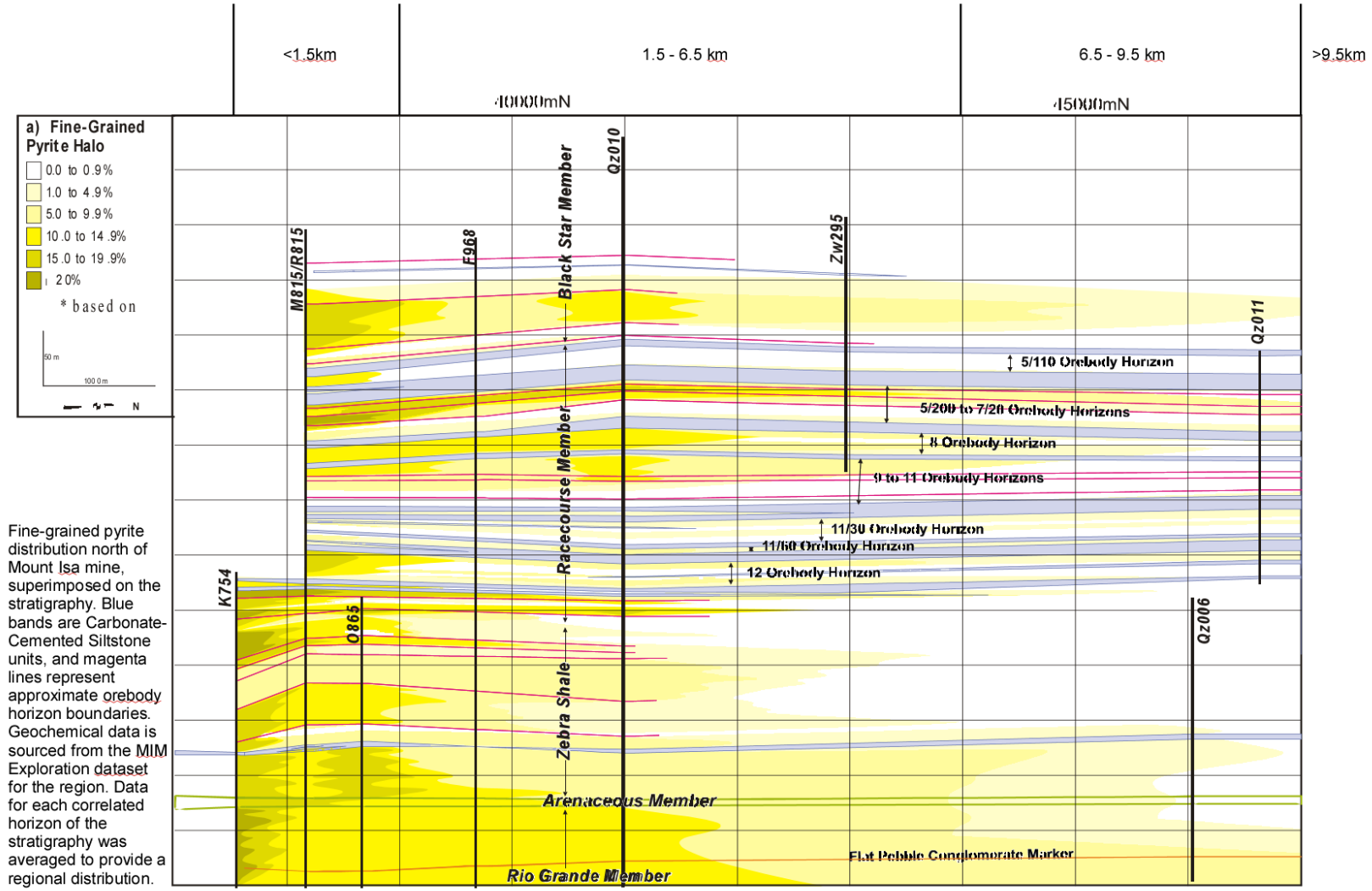

Fine-grained pyrite distribution north of Mount Isa mine, superimposed on the stratigraphy. Blue bands are Carbonate-Cemented Siltstone units, and magenta lines represent approximate orebody horizon boundaries. Geochemical data is sourced from the MIM Exploration dataset for the region. Data for each correlated horizon of the stratigraphy was averaged to provide a regional distribution.

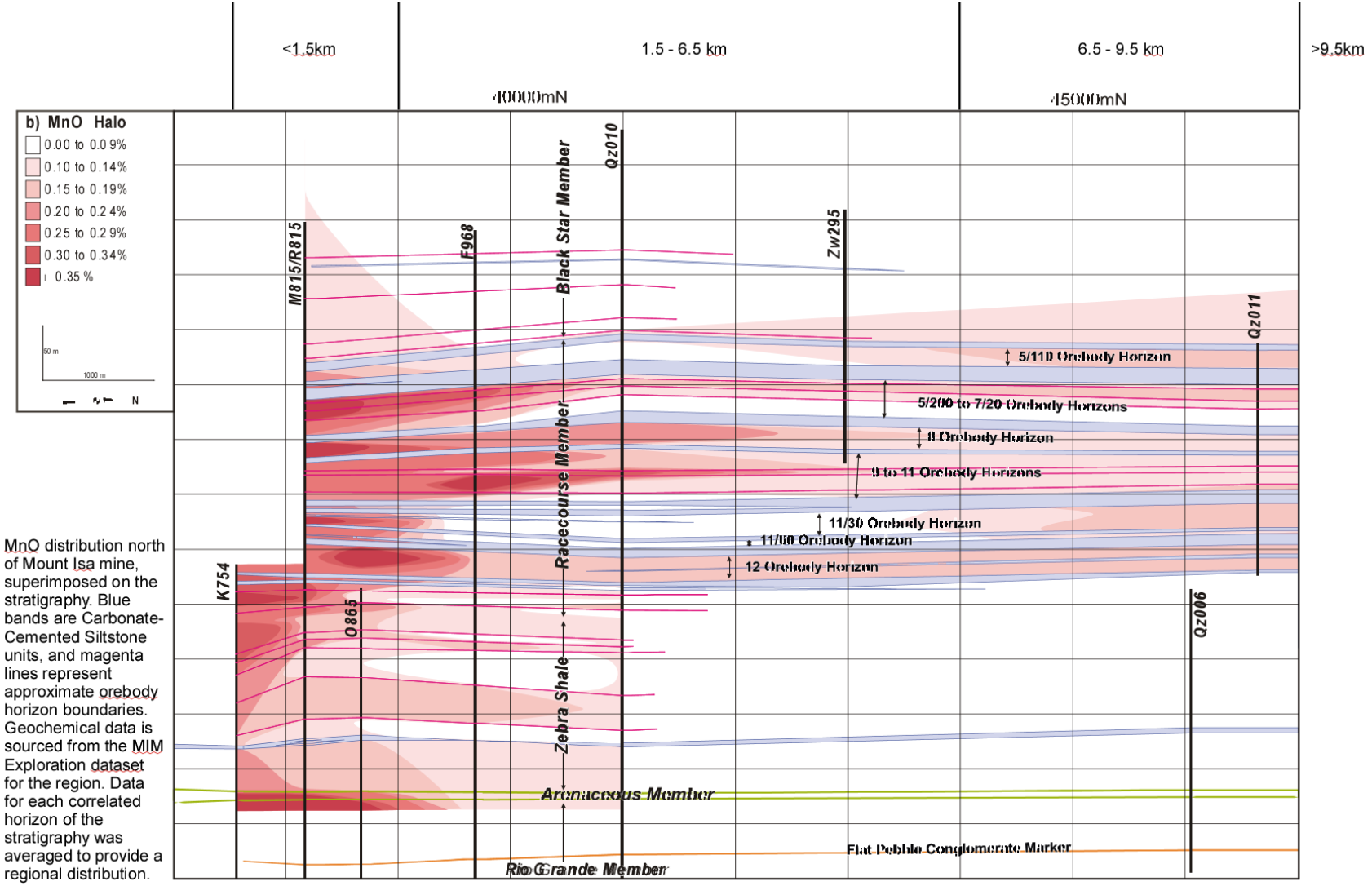

MnO distribution north of Mount Isa mine, superimposed on the stratigraphy. Blue bands are Carbonate-Cemented Siltstone units, and magenta lines represent approximate orebody horizon boundaries. Geochemical data is sourced from the MIM Exploration dataset for the region. Data for each correlated horizon of the stratigraphy was averaged to provide a regional distribution.

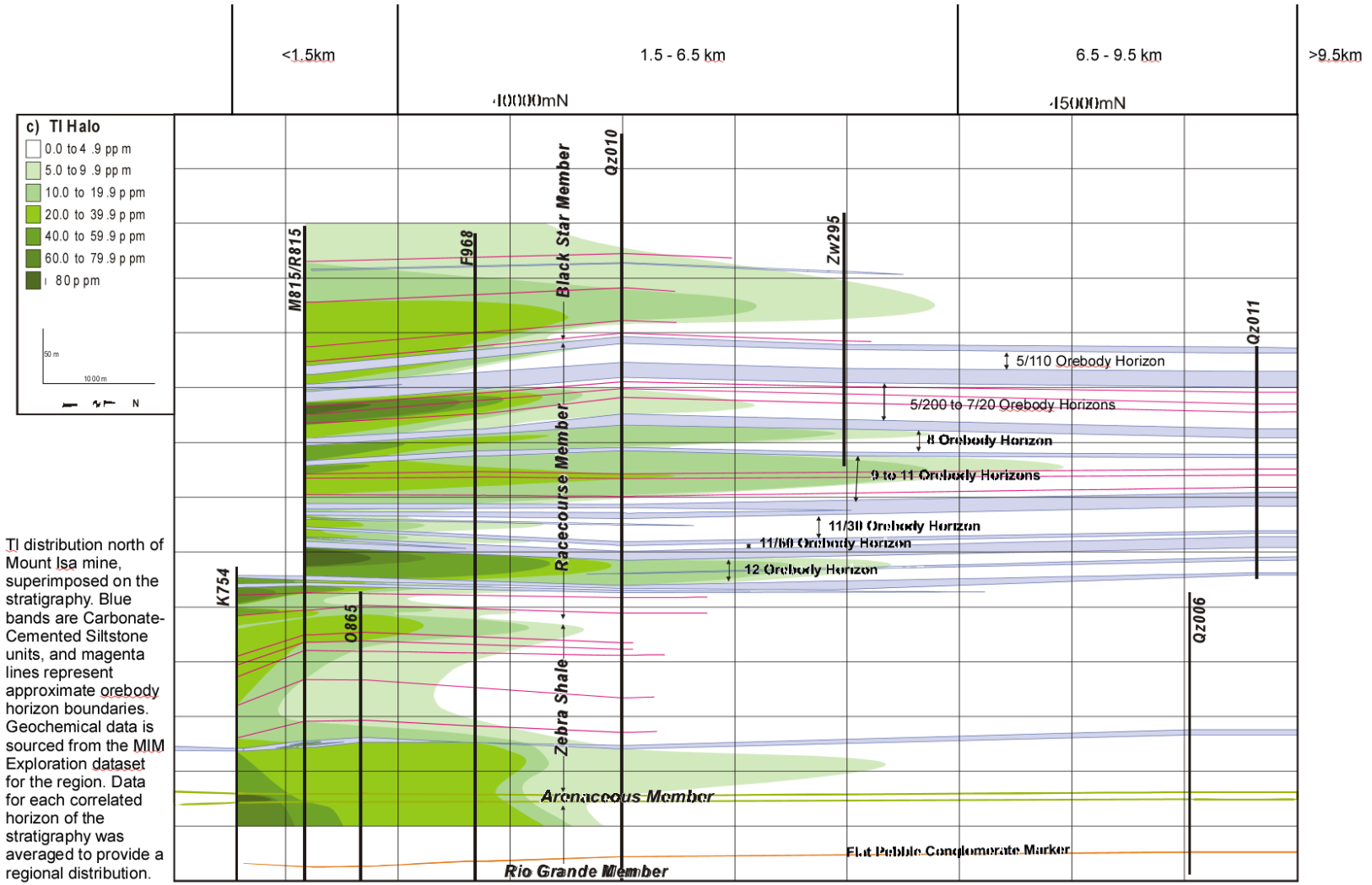

Tl distribution north of Mount Isa mine, superimposed on the stratigraphy. Blue bands are Carbonate-Cemented Siltstone units, and magenta lines represent approximate orebody horizon boundaries. Geochemical data is sourced from the MIM Exploration dataset for the region. Data for each correlated horizon of the stratigraphy was averaged to provide a regional distribution.

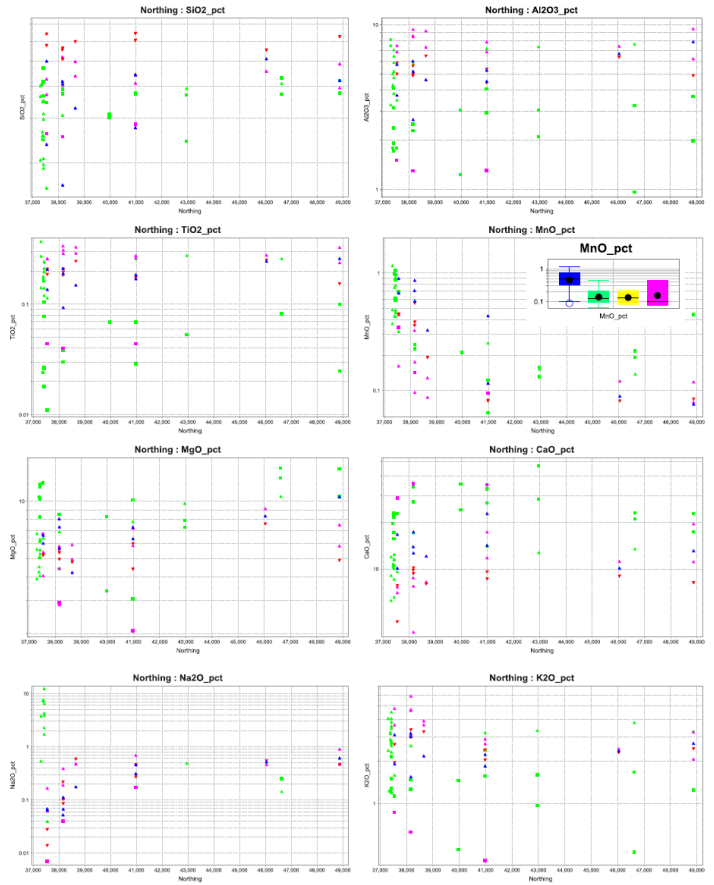

Figure 2.28 (this page, facing page and subsequent 2 pages). Elemental plots of analyses reported by Painter (2003), showing the variation in chemistry within the Urquhart Shale as a function of northing (Isa lease regional grid). The left hand side of each plot represents the northern end of the Isa mine Pb-Zn-Ag orebodies, and plotted results cover a distance of approximately 11km to the north of economic mineralisation within the same stratigraphic interval. Inset maps show box and whisker plots of data sorted into distance categories as shown in the legend. Individual elements and indices are discussed further in the halo section of the text.

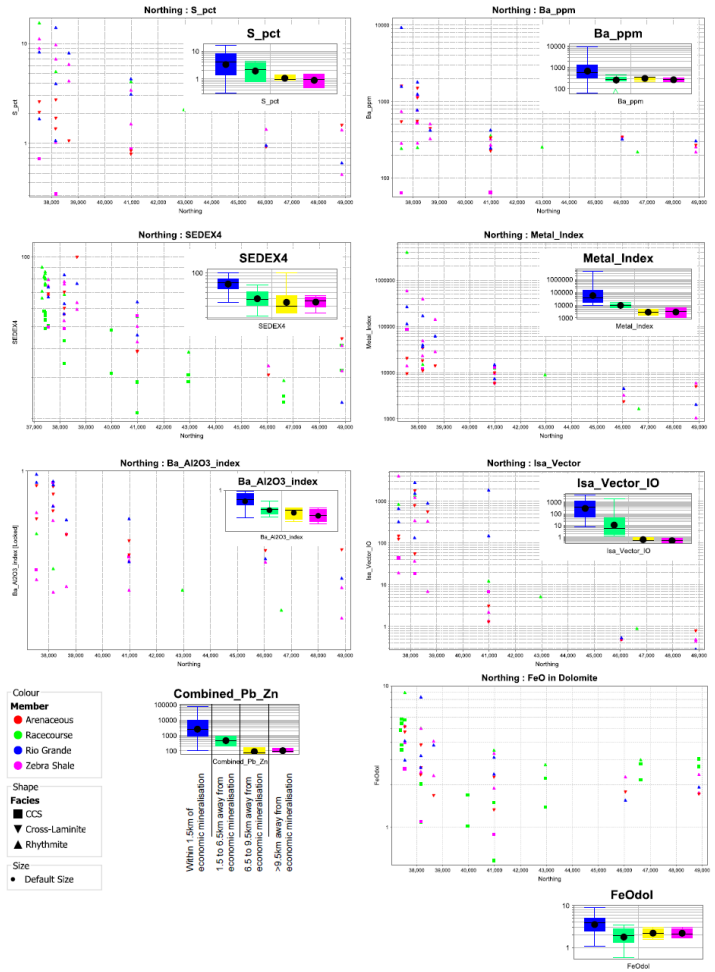

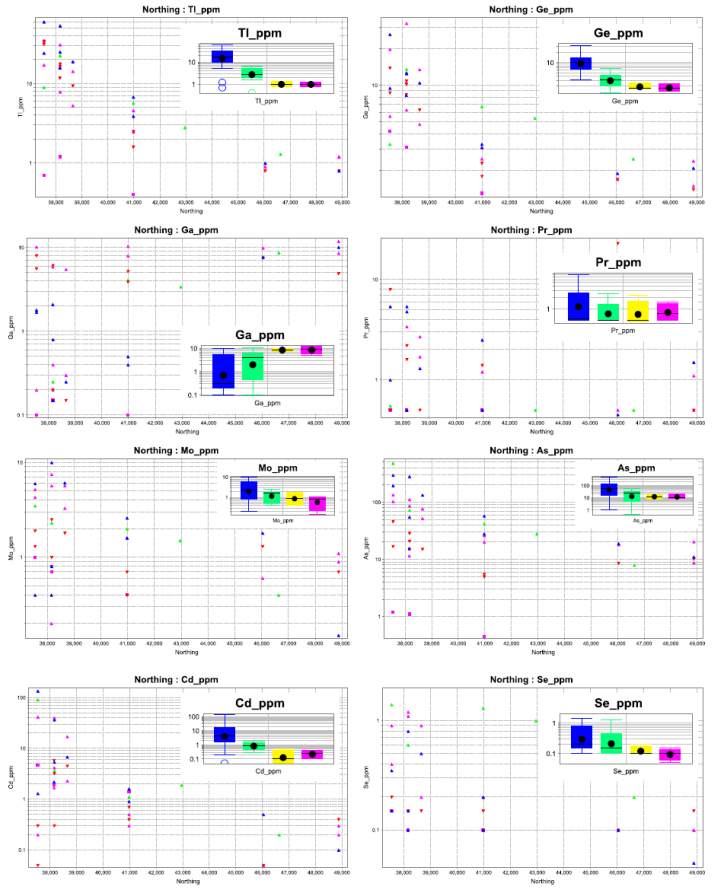

Figure 2.28 (cont'd) (this page, facing page and previous2 pages). Elemental plots of analyses reported by Painter (2003), showing the variation in chemistry within the Urquhart Shale as a function of northing (Isa lease regional grid). The left hand side of each plot represents the northern end of the Isa mine Pb-Zn-Ag orebodies, and plotted results cover a distance of approximately 11km to the north of economic mineralisation within the same stratigraphic interval. Inset maps show box and whisker plots of data sorted into distance categories as shown in the legend. Individual elements and indices are discussed further in the halo section of the text.

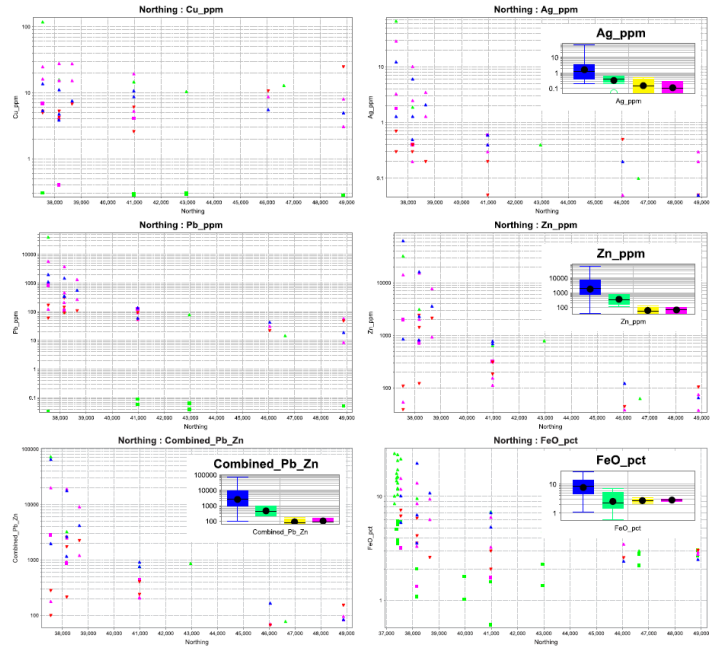


SiO2_pct
TiO2_pct
Al2O3_pct
FeO_pct
MnO_pct
MgO_pct
CaO_pct
Na2O_pct
K2O_pct
P2O5_pct
S_pct
Ba_ppm
Rb_ppm
Sr_ppm
Y_ppm
Zr_ppm
Nb_ppm
Th_ppm
Pb_ppm
Zn_ppm
Ag_ppm
Tl_ppm
Ga_ppm
Cu_ppm
Ni_ppm
V_ppm
Cr_ppm
Cd_ppm
Ge_ppm
As_ppm
Se_ppm
Sb_ppm
Br_ppm
Hf_ppm
Cs_ppm
Ta_ppm
Co_ppm
U_ppm
W_ppm
Sn_ppm
Mo_ppm
La_ppm
Ce_ppm
Pr_ppm
Nd_ppm
SEDEX4
Metal_Index
Ba_Al2O3_index
Isa_Vector_IO
Combined_Pb_Zn
Legend
Colour
Northing Distance
Northing to 39000 [63.01
Northing to 44000 [83.56
Northing to 47000 [91.78
Northing to ? [100.00%]

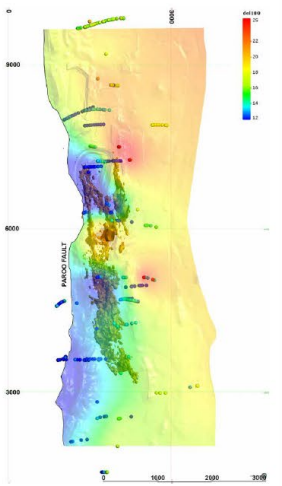

Figure 2.29. Colour gradation of $\delta^{18}O$ evaluated on the local DTM surface, showing an approximation of the expected pattern of $\delta^{18}O$ from shallow drilling. Data from the pmd*CRC I4 project compilation based on Waring (1990) stable isotope data..

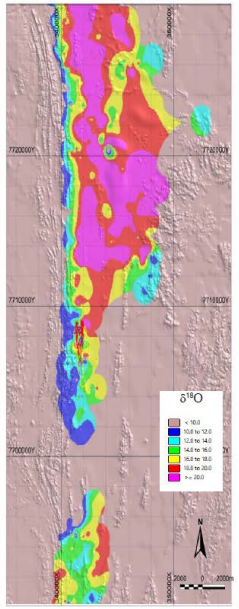

Figure 2.30. Regional pattern of $\delta^{18}O$ with all values projected to surface, showing a complex pattern but also showing a $\delta^{18}O$ depletion around and to the south of the mine. Data from the pmd*CRC I4 project compilation based on Waring (1990) stable isotope data..

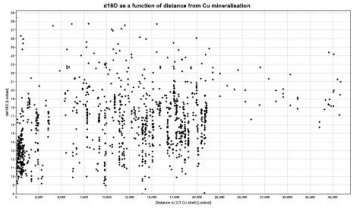

Figure 2.31. X-Y plot of $\delta^{18}O$ plotted against distance from the 2% copper shell, showing a depleted zone near the copper orebodies but also highlighting the existence of low $\delta^{18}O$ values in samples at a significant distance from copper mineralization. Data from the pmd*CRC I4 project compilation based on Waring (1990) stable isotope data..

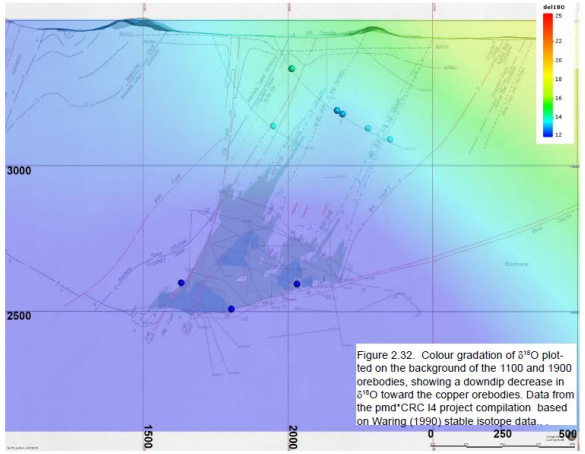

Figure 2.32. Colour gradation of $\delta^{18}O$ plotted on the background of the 1100 and 1900 orebodies, showing a downdip decrease in $\delta^{18}O$ toward the copper orebodies. Data from the pmd*CRC I4 project compilation based on Waring (1990) stable isotope data..

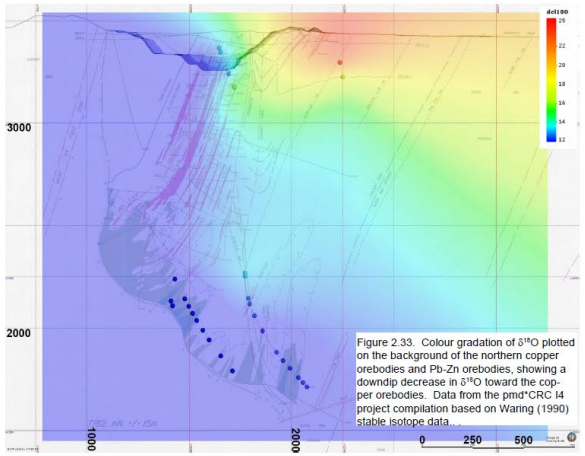

Figure 2.33. Colour gradation of $\delta^{18}O$ plotted on the background of the northern copper orebodies and Pb-Zn orebodies, showing a downdip decrease in $\delta^{18}O$ toward the copper orebodies. Data from the pmd*CRC I4 project compilation based on Waring (1990) stable isotope data..

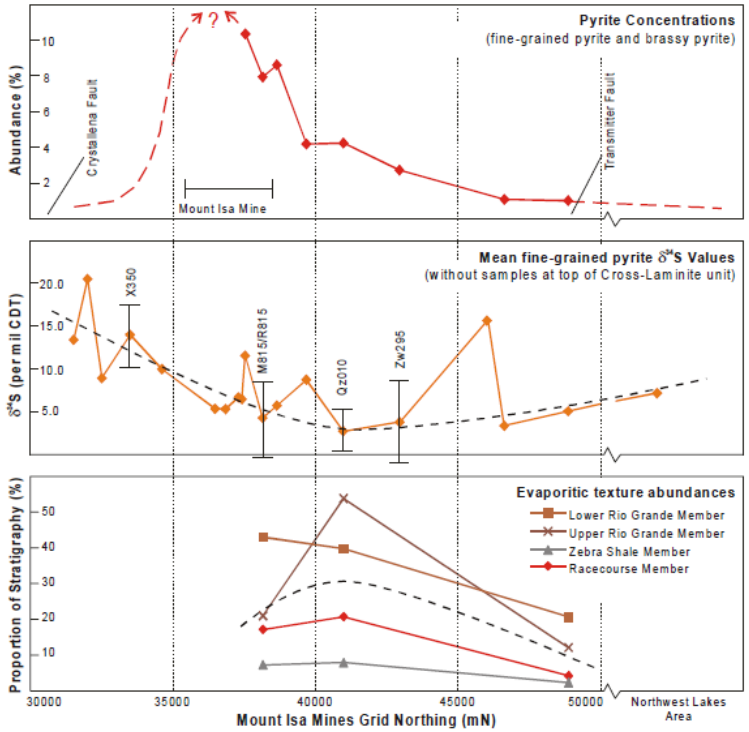

Figure 8.03 - Comparison of spatial distributions for pyrite abundances, fine-grained pyrite sulfur isotope values and evaporitic abundances. All values plotted represent average values per northing. 1. Pyrite abundances - solid line represents plotted data , dashed line is an estimate from drill core logs. Note the positions of the Crystallena and Transmitter Faults and the Mount Isa Mine. 2. Average fine-grained pyrite sulfur isotope distribution - finely dashed line represents trend of the isotopic data. Sample from the top of the Arenaceous Member were excluded as most northern samples were from around this horizon, giving a false impression of enhanced enrichment north of 45000mN. 3. Evaporitic texture abundances - as determined from sedimentological logs. Peaks in evaporitic texture abundances are in Qz010 for 3 of the 4 stratigraphic members.

Painter, 2003

Isa Zoning Summary

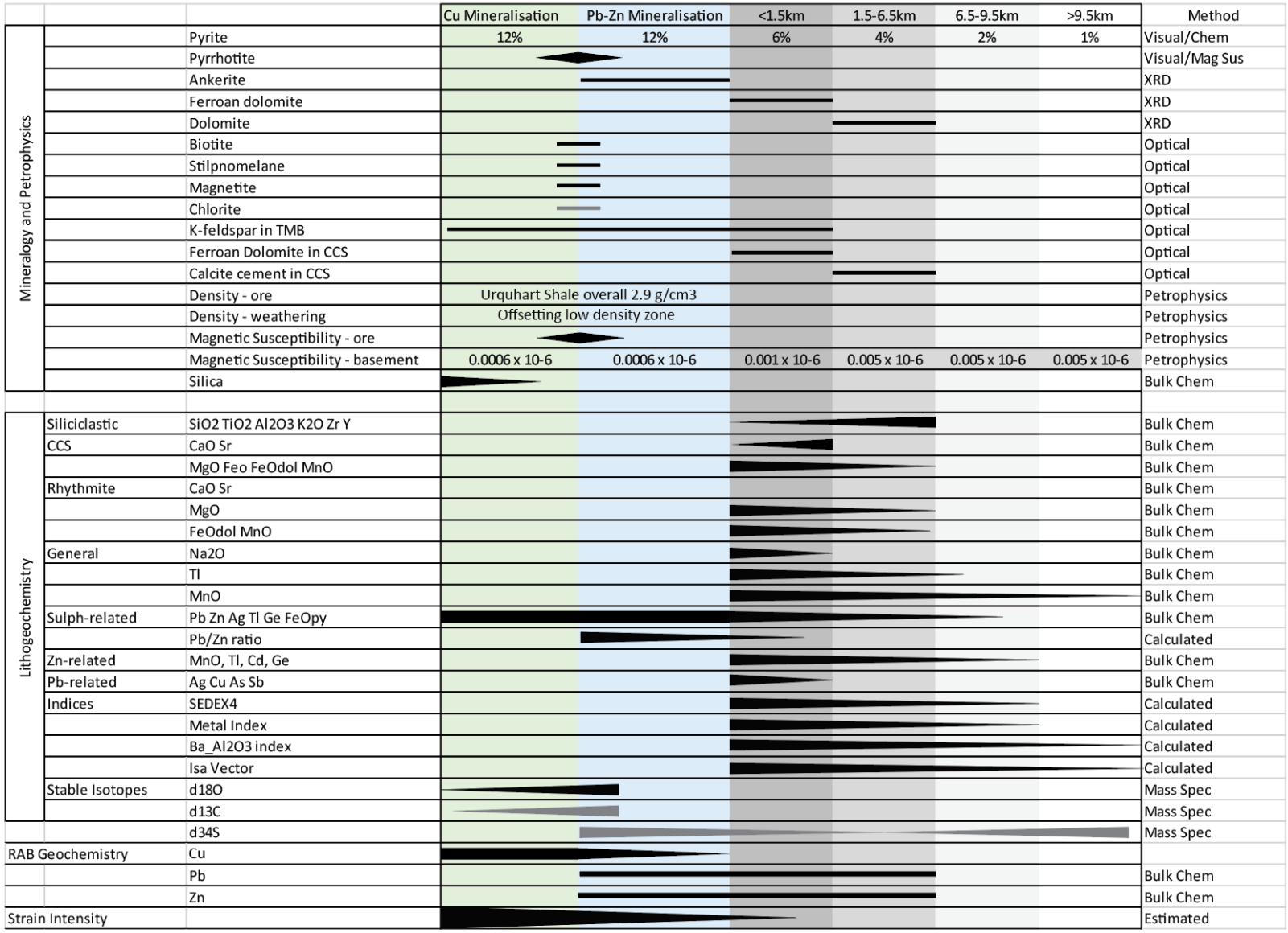

>9.5km

MnO; Ba Al2O3 index; Isa vector; pyrite

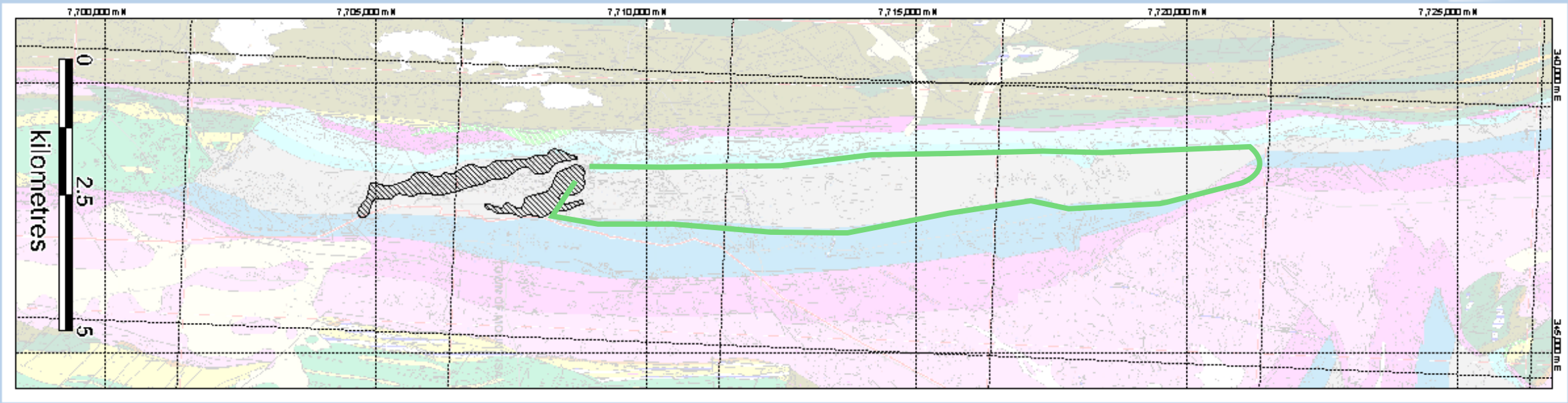

6.5-9.5km

SEDEX4 Index; Metal index; Thallium halo; Pb+Zn

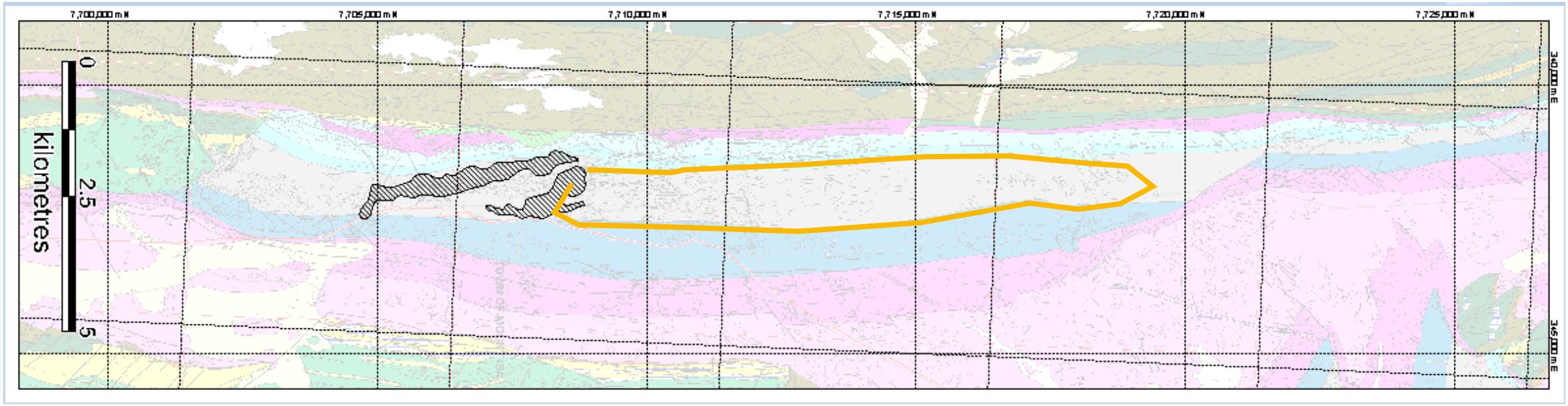

1.5-6.5km

Pb Zn geochemistry; MgO; FeO; FeOdol;

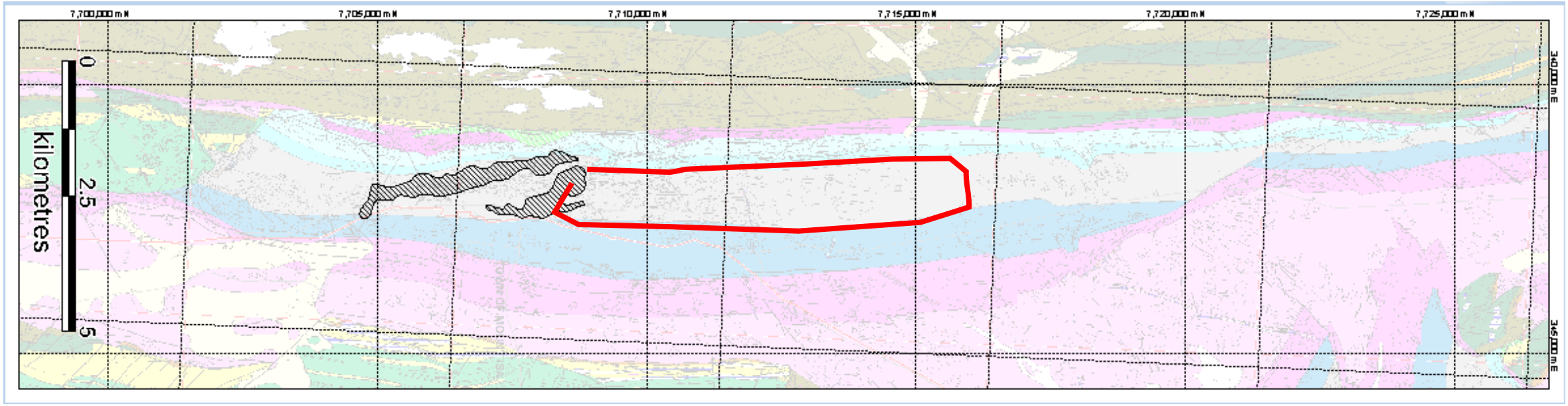

>1.5km

K2O halo; Ferroan dolomite cement; Cu rab; CaO in CCS; Pb suite; strain intensity

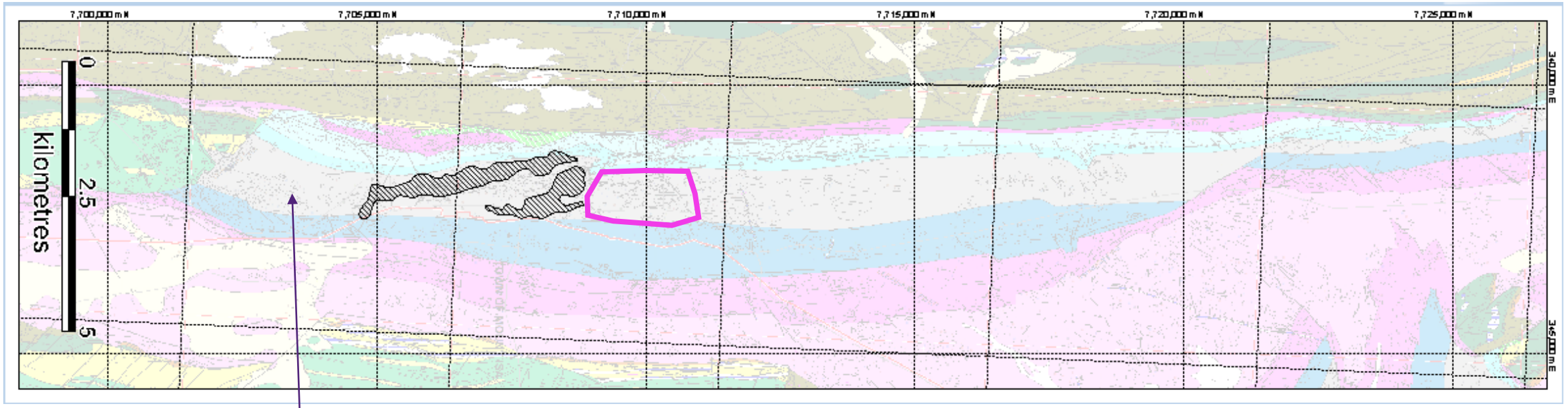

Cu also extends to south